Indian J Microbiol (Apr–June 2018) 58(2):214–221
https://doi.org/10.1007/s12088-018-0710-8

ORIGINAL RESEARCH ARTICLE

Extracellular Synthesis and Characterization of Gold Nanoparticles Using *Mycobacterium* sp. BRS2A-AR2 Isolated from the Aerial Roots of the Ghanaian Mangrove Plant, *Rhizophora racemosa*

Mustafa Camas[1] · Anil Sazak Camas[1] · Kwaku Kyeremeh[2]

Received: 6 December 2017 / Accepted: 13 January 2018 / Published online: 22 January 2018

Abstract Through the use of genomes that have undergone millions of years of evolution, marine *Actinobacteria* are known to have adapted to rapidly changing environmental pressures. The result is a huge chemical and biological diversity among marine *Actinobacteria*. It is gradually becoming a known fact that, marine *Actinobacteria* have the capability to produce nanoparticles which have reasonable sizes and structures with possible applications in biotechnology and pharmacology. *Mycobacterium* sp. BRS2A-AR2 was isolated from the aerial roots of the mangrove plant *Rhizophora racemosa*. The *Mycobacterium* was demonstrated for the first time ever to produce AuNPs with sizes that range between 5 and 55 nm. The highest level absorbance of the biosynthesized AuNPs was typical for actinobacterial strains (2.881 at 545 nm). The polydispersity index was measured as 0.207 in DLS and the zeta potential was negatively charged (− 28.3 mV). Significant vibration stretches were seen at 3314, 2358, 1635 and 667 cm^{-1} in FT-IR spectra. This demonstrated the possible use of small aliphatic compounds containing –COOH, –OH, –Cl and $–NH_2$ functional groups in the stabilization of the AuNPs. The effect of the biosynthesized AuNPs on HUVEC and HeLA cell lines was measured at 48 h. IC_{50} values were determined at 3500 µg/ml concentration for HUVEC and HeLA cell lines at 45.25 and 53.41% respectively.

Keywords Actinobacteria · Gold nanoparticles · Cytotoxicity · Spectroscopy

Introduction

Nanoparticles are attractive materials for industrial and biomedical applications because of their unique features such as high surface area and porosity [1, 2]. Metal nanoparticles have diverse applications especially in the biological fields where they are used in diagnostics and therapeutics [3], electronics and photonics [4], pharmaceuticals [5], biofuels [6], optics and optoelectronics [7, 8] and nanocomposites [9, 10]. Amongst metal nanoparticles, the biosynthesis of gold nanoparticles has gained extensive consideration as one of the major frontiers of scientific research in the current years due to their profound biocompatibility. Gold nanoparticles with different shapes and sizes produced by diverse microorganisms perform numerous functions which are associated with many applications in the field of medicine, for example, diagnosis and therapy in cancer treatment, as potent antiangiogenic and antiarthritic agents and antimalarials. For instance, nanocomposites of Ag-graphene, Au-graphene or Au-SnO_2 have been developed for electrochemically active biofilms (EABs) and help in the bio-reduction of gold nanoparticles without the need to use capping or surfactants [11]. These nanocomposites have various applications including their use as sensors, photoelectrodes, optoelectronic devices, photocatalysis, photovoltaic, ultracapacitors and photovoltaics. Nanocomposites are extremely

Electronic supplementary material The online version of this article (https://doi.org/10.1007/s12088-018-0710-8) contains supplementary material, which is available to authorized users.

✉ Mustafa Camas
mustafacamas@gmail.com

[1] Department of Bioengineering, Munzur University, 62000 Tunceli, Turkey

[2] Department of Chemistry, School of Physical and Mathematical Sciences, University of Ghana, P.O. Box LG 56, Legon-Accra, Ghana

remarkable due to their excellent photoelectrochemical and photocatalytic properties [12, 13].

Gold nanoparticles have been previously synthesized through basic physical and synthetic techniques by utilizing a complicated blend of hazardous chemicals and radioactive substances. Lately, eco-accommodating techniques for the biosynthesis of gold nanoparticles have reduced cost and resulted in focus on natural combinations of such nanoparticles [14]. Previous research has demonstrated the ability of gold nanoparticles to interact effectively with proteins through hydrogen bonding, dipole–dipole interactions and covalent bonding. These interactions are facilitated by free amine groups or cysteine residues which are common side groups along the tertiary structure of proteins. Proteins that reduce chloroaurate ions and cap the gold nanoparticles delivered by the diminishment procedure may have a place as discharged catalysts. Along these lines, it is gradually becoming a well-known fact that capping and stabilization of gold nanoparticles can be achieved by different proteins. Numerous effective research endeavours have been made for different combinations of metal nanoparticles utilized by actinobacteria, fungi, algae, yeast, cyanobacteria, and plants [15]. Prokaryotic bacteria have been researched for their ability to produce a broad blend of metallic nanoparticles. One reason for "bacterial inclination" for nanoparticles synthesis is their relative simplicity and control [16]. *Actinobacteria* have proved an extremely viable source of novel secondary metabolites, for example, antibiotics, immunosuppressants, and numerous other biologically active compounds [17]. Currently, the marine environment has proved to be a tremendous source of many different species of *Actinobacteria* whose genetic composition has undergone many years of evolution. The genetic composition of marine *Actinobacteria* therefore constitute a huge biological and chemical diversity resource which has already provided our clinics with new drug entities. Interesting marine *Actinobacteria* show broad distribution in tidal zones [18], seawater [19], animals [20], sponges [21] and marine sediments [22]. Amongst the many different applications of materials from marine *Actinobacteria*, there is also the need to further explore and understand their ability to synthesise metallic nanoparticles. The ability of marine *Actinobacteria* to biosynthesize appropriate nano-sized nanoparticles could find important applications in the pharmaceutical and biotechnological industries [1]. However, until now, gold nanoparticle synthesis from marine *Actinobacteria* has been reported only for *Streptomyces* sp. LK-3 [23], *Streptomyces* sp. MBRC-82 [24] and *Nocardiopsis* sp. MBRC-48 [25]. *Mycobacteria* are members of the *Actinobacteria* with characteristic rod-shapes and are mostly Gram-positive aerobes or Facultative anaerobes. It is thought that, the more well-known infectious agents such as *Mycobacterium tuberculosis* and *Mycobacterium leprae* have evolved from soil bacteria and produce some of the most devastating clinical conditions known to man. Currently, gold nanoparticles have been investigated as possible antimycobacterial agents or mediators for antimycobacterial agents [26] and also as biosensors for detection *M. tuberculosis* [27].

This report describes for the first time ever, the biosynthesis, characterization and cytotoxicity effects on HUVEC and HeLA cell lines of gold nanoparticles produced by *Mycobacterium* sp. BRS2A-AR2 (KT945161) which was isolated from the roots of the Ghanaian mangrove plant *Rhizophora racemosa* collected from the banks of the Butre River in the Western Regional Wetlands of Ghana.

Materials and Methods

Mangrove Plant Sample Collection

The Western Region of Ghana is noted for its bio-diversely rich indigenous mangrove plants. Out of the six indigenous plants that are characteristic of the mangroves found in Ghana, three of them are particularly common in the Western Region and these are *Conocarpus erectus*, *Laguncularia racemosa* and *Rhizophora racemosa* (coordinates: 4°49′43.73′N and 1°54′50.84′W). Collection of mangrove plants was done along the banks of the River Butre with five sampling sites chosen at 100 m apart from the shore to where the river meets the sea. The three main plant samples collected were *Conocarpus erectus*, *Laguncularia racemosa* and *Rhizophora racemosa* but, different plant parts were sampled at different sections of the river. The plant parts sampled were leaves, buds, submerged roots, aerial roots, aerial stems, fruit shoots and flowers. The exact positions of plants from which different parts were sampled were stored in a GPS and the data uploaded into Google Earth satellite database. The samples were videoed, photographed, bagged, labelled and stored at 4 °C in an ice-chest and transported to the Department of Chemistry, University of Ghana, Legon. Identification of the plants was done at the Department and specimens of all plant parts collected were dried in newspapers for onward submission to the herbarium.

Treatment of *Rhizophora racemosa* and Culture of BRS2A-AR2

In the laboratory, pieces of the aerial roots of *Rhizophora racemosa* were surface sterilized under sterile conditions by first rinsing them with sterile artificial sea water (SASW) and then immersing them in 70% ethanol for

1 min. The plant parts were then cut transversely at all sides into a smaller piece with a pair of flame sterilized scissors in a bio-safety cabinet. The pieces were again sterilized under sterile conditions by first rinsing them with SASW and then immersing them in 70% ethanol for 1 min. The pieces were again cut at all sides into much smaller pieces with a flame sterilized scalpel. These pieces were again sterilized by rinsing with SASW, then immersing in 2% sodium hypochlorite for 1 min and then rinsed again with SASW 3 times. The treated aerial roots were afterwards placed on malt extract agar plates (parent or master plates) and the plates were labelled, parafilmed and incubated at 28 °C for 3 weeks with daily observations to detect the appearance of new putative actinobacterial colonies.

Isolation of Pure BRS2A-AR2

Observation of the parent or master plates obtained for the aerial roots of *Rhizophora racemosa* starting from day one to day twenty-one saw the appearance on the parent plates of several different colonies of marine actinobacteria which were subsequently picked one at a time, re-cultured on fresh malt extract plates and kept at an incubation temperature of 28 °C. All the colonies initially sub-cultured from the parent or master plates were subsequently sub-cultured until very pure strains were obtained for each species, one of which was the isolate BRS2A-AR2.

Biosynthesis of Gold Nanoparticles

For gold nanoparticles biosynthesis, the isolate BRS2A-AR2 was incubated for 5 days in ISP2 medium and fermentation was performed at 28 °C at 180 rpm for 72 h in a shaking incubator. After incubation, the cell-free supernatant of isolate was centrifuged at 4000 rpm for 30 min and furthermore maintained at +4 °C in sterile glass bottles. The acquired upper phase was incubated with close monitoring of the colour changes in 24 h at 35 °C in the dark with a mix of 1/9 percent 1×10^{-3} M Gold (III) chloride trihydrate ($HAuCl_4 \cdot 3H_2O$, Sigma-Germany) [28]. After observing the color change of the centrifuged isolate at 24 h, the mixture was again incubated at 4000 rpm for 15 min., the absorbance values in the wavelength range 400–800 nm were recorded using the Optima SP-3000 UV–VIS spectrophotometer.

Identification of the Isolate BRS2A-AR2 Based on 16S rRNA Gene Region

The isolate BRS2A-AR2 that was found to biosynthesize gold nanoparticles through the measurement of UV–VIS spectrophotometric absorbance data was identified based on the 16S rRNA gene. The genomic DNA of isolates was extracted with a DNA bacterial/fungal extraction kit according to the manufacturer's protocol (Zymo Research, USA), and the 16S rRNA gene was amplified by using universal bacterial 16S rRNA primers 27F and 1525R [29]. The PCR product was purified using a PCR purification kit, and direct sequence determination of the purified 16S rRNA gene was performed using universal sequencing primers 518F and 800R with an Applied Biosystems automated sequencer. Identification of the closest phylogenetic neighbors and calculation of pairwise 16S rRNA gene sequence similarities were achieved using the EzTaxon-e server (http://eztaxon-e.ezbiocloud.net; [30]). The MEGA6 program was used for phylogenetic analysis, and the Clustal-W option in the same program was used for alignment [31]. Phylogenetic trees were inferred using the neighbor-joining [32], maximum-parsimony [33] and maximum-likelihood [34] algorithms. Evolutionary distances were calculated using the Jukes & Cantor model. Topologies of the resultant trees were evaluated by bootstrap analysis [35] based on 1000 re-samplings.

Fourier Transform Infrared Spectroscopy (FT-IR)

FTIR can be valuable for preparatory examination of surface chemistry of biosynthesized nanoparticles. IRAffinity-1S Fourier Transform Infrared Spectrophotometer (Shimadzu, Japan) was used for FT-IR analysis. Characterization of the functional groups of AuNPs synthesized by the strain BRS2A-AR2 was determined at a resolution in the range of 400–4000 cm^{-1}.

Dynamic Light Scattering (DLS), Zeta Potential (ZP) and TEM Imaging

AuNPs were analyzed in DTS0012 sizing cuvette with an optical path length of 1 cm at 25 °C for DLS. 630 µl of AuNP sample was analyzed using DTS1060C—Clear dispensable zeta cell at 25 °C for zeta potential. Measurement of the size (DLS) and zeta potential (surface charge) of gold colloidal particles was carried out using Zetasizer Nano Series (Nao-ZS), Malvern Instruments Ltd. (Malvern, UK). The TEM images of Au-NPs were determined at 120 kV.

Cytotoxicity and Anti-carcinogenicity Effects of AuNPs

Cytotoxic effects on the living Human umbilical vein endothelial cell line (HUVEC) and anticarcinogenic effects on Human Cervical Cancer (HeLA) cell line of biosynthesized AuNPs from *Mycobacterium* sp. BRS2A-AR2 were carried out using the [(3-(4,5-Dimethylthiazol-2-yl)-2,5-Diphenyltetrazolium Bromide] (MTT) test for 24 and

48 h exposure times. Cultures were maintained in Eagle's Minimum Essential Medium with foetal bovine serum to a final concentration of 10%. Cells were kept in 95% humidity, 5% CO_2 at 37 °C. Exponentially growing cells were plated in a 96 well microtitre plate at a uniform cell density of 5×10^3 cells/well 24 h before treatment. Cells were treated with the varying concentrations of AuNPs for various time intervals 24 h and 48 h before the MTT assays were performed. At the end of treatment, control and treated cells were incubated with MTT at a final concentration of 0.05 mg/mL for 2 h at 37 °C after which the medium was removed. The cells were lysed and the formazan crystals were dissolved using 150 µL of dimethylsulfoxide. Optical density was measured on 150 µL of extracts at 570 nm. Triton X-100 (0.5%) was measured as positive control. The formula used to calculate % viability is as shown below.

$$\% \text{ of viability} = [OD_{570-630nm} \text{ test product}/OD_{570-630nm} \text{ control}] \times 100\%$$

Results

The strain *Mycobacterium* sp. BRS2A-AR2 used in the present study was isolated from the aerial roots of *Rhizophora racemosa* and sub-cultured on malt extract agar until pure. Yellowish orange, viscous, and non-spore forming colonies were purified in ISP2 agar medium (Fig. 1). An almost-complete 16S rRNA gene sequence (1440 nt) of strain BRS2A-AR2 determined in this study was compared with the corresponding sequences of members of the genus *Mycobacterium.* The phylogenetic tree based on the neighbor-joining algorithm showed that strain BRS2A-AR2 formed a distinct branch from other *Mycobacterium* species, notably from its nearest neighbors (Fig. 2). Sequence similarity of identity calculations indicated that the closest relatives of strain BRS2A-AR2 were *Mycobacterium houstonense* ATCC 49403^T (99.1%; 12 nt differences at 1440 locations) and *Mycobacterium senegalense* AY457081^T (99.1%; 12 nt differences at 1440 locations).

Fig. 1 The strain BRS2A-AR2 isolated mangrove plants from The Western Region of Ghana

Gold nanoparticles display characteristic optical absorption spectra in the UV–Visible region. The UV–Vis spectra recorded for the chloroauric acid and cell free extract of *Mycobacterium* sp. BRS2A-AR2 was in maintaining media. After reaction period, the mixture turned into a dark pinkish colour. Maximum absorbance at 545 nm wavelength was determined as 2.881 (Fig. 3a). Fourier Transform Infrared Spectroscopy (FT-IR) is widely used for the identification of functional groups such as amines, carbonyls and hydroxyls that are found within the structures of many molecules. The FTIR spectrum of the biosynthesized gold nanoparticles showed characteristic bands at 3314, 2358, 1635 and 667 cm^{-1} in Fig. 3b. The peak at 3314 cm^{-1} corresponds to O–H group of phenolic and alcoholic molecules but, since the spectrum shows no further signs of the presence of an aromatic compound, this completely rules out phenols. The absorption band at 2358 cm^{-1} was assigned to dissolved CO_2 which is known to show this peak in the presence of traces of water. The peak in the region of 1635 cm^{-1} can be assigned to a carbonyl group connected to an atom that possess lone pairs of electrons and is less electronegative compared to oxygen. In this instance, resonance structures which convert the C=O bond into C–O– can disrupt the integrity of the C=O and result in lower vibrational stretch frequencies for this functional group. The peak at 1635 cm^{-1} can be assigned therefore to an amide [36]. The peak located at 667 cm^{-1} is strong and broad and can be assigned to C–Cl stretching in aliphatic organic compounds, since for aromatic compounds, this peak is mostly absent. Unfortunately, the width of the IR spectra 400–4000 cm^{-1} does not allow the C–Cl deformations that normally appear below 400 cm^{-1} to be seen. [37]. Dynamic light scattering spectroscopy is a procedure that makes it possible to gauge the size and size appropriation of nanoparticles when dissolved in a liquid. Investigation of laser diffraction uncovered that the acquired AuNPs demonstrated the Z-average value (d.nm) (average gold nanoparticle size) and the polydispersity index (PDI) value are 153.5 nm and 0.207 respectively (Fig. 3c). Zeta potential is a good indicator of the repulsion forces between particles and is used to estimate the stability of nanoparticles in the media. The zeta potential of the gold nanoparticles is − 28.3 mV which compares to the negatively charged gold nanoparticles (Fig. 3d).

TEM incorporates high caliber, detailed and capable amplification of component and compound structures. The TEM micrograph shows representation of the gold

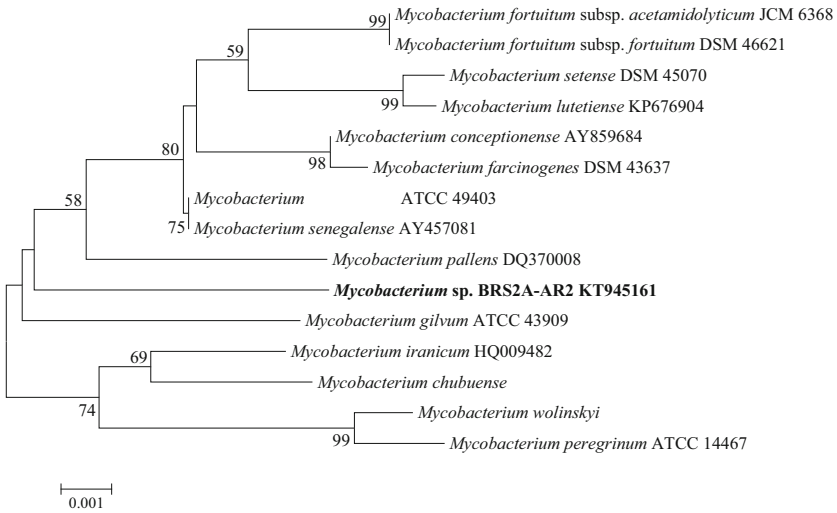

Fig. 2 Phylogenetic tree based on 16S rRNA gene sequences showing the relationships of *Mycobacterium* sp. BRS2A-AR2 and related taxa. The dendrogram was reconstructed by using the neighbor-joining method. Bootstrap values (based on 1000 replicates) greater than 50% are shown at nodes. Bar, 0.001 sequence dissimilarity per nucleotide position. GenBank ID: KT945161

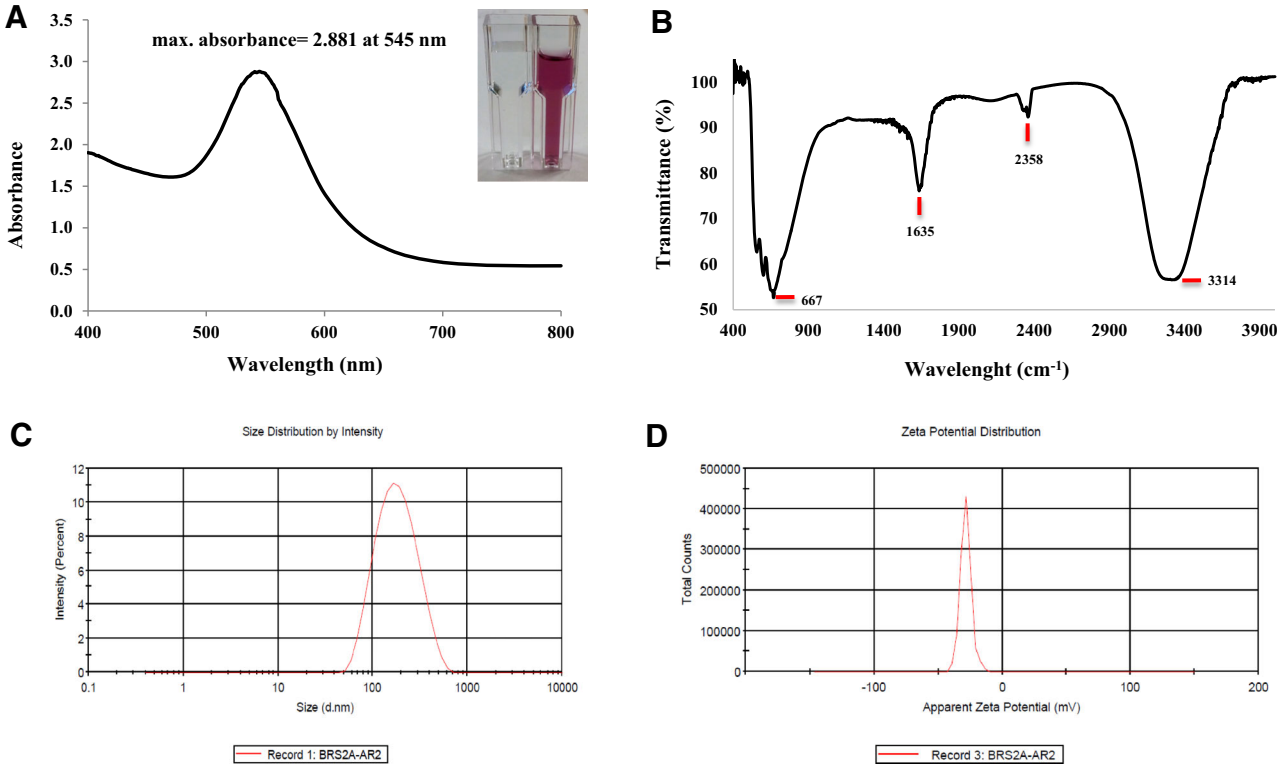

Fig. 3 Images of gold nanoparticles using the strain BRS2A-AR2. **a** UV–VIS spectra; **b** FT-IR, **c** size distribution with DLS; **d** zeta potential distribution

nanoparticles utilizing the supernatant of *Mycobacterium* sp. BRS2A-AR2 (Fig. 4a). The particles were framed in various sizes, ranging from 5 to 55 nm in diameter, scattered in little and expansive round shapes (Fig. 4b). Average particle size was 11.8 nm.

The cytotoxic effects of the biosynthesized gold nanoparticles on HUVEC cell lines and anticarcinogenic effects on HeLA cell lines of biosynthesized AuNPs after 24 and 48 h of reaction were evaluated. After 24 h of reaction, cytotoxic effets of AuNPs in all doses was considered statistically non-significant on HUVEC cell lines. However, AuNPs caused cytotoxicity by reducing cell viability at all doses (except 875 µg/mL) in a period of 48 h and the IC_{50} value was 45.25% at 3500 µg/ml concentration. AuNPs were found to increase anticarcinogenic effects on HeLA cell lines for high doses especially at 24 and 48 h of reaction with IC_{50} value of 53.41% at 3500 µg/ml concentration (Supp. Table 1).

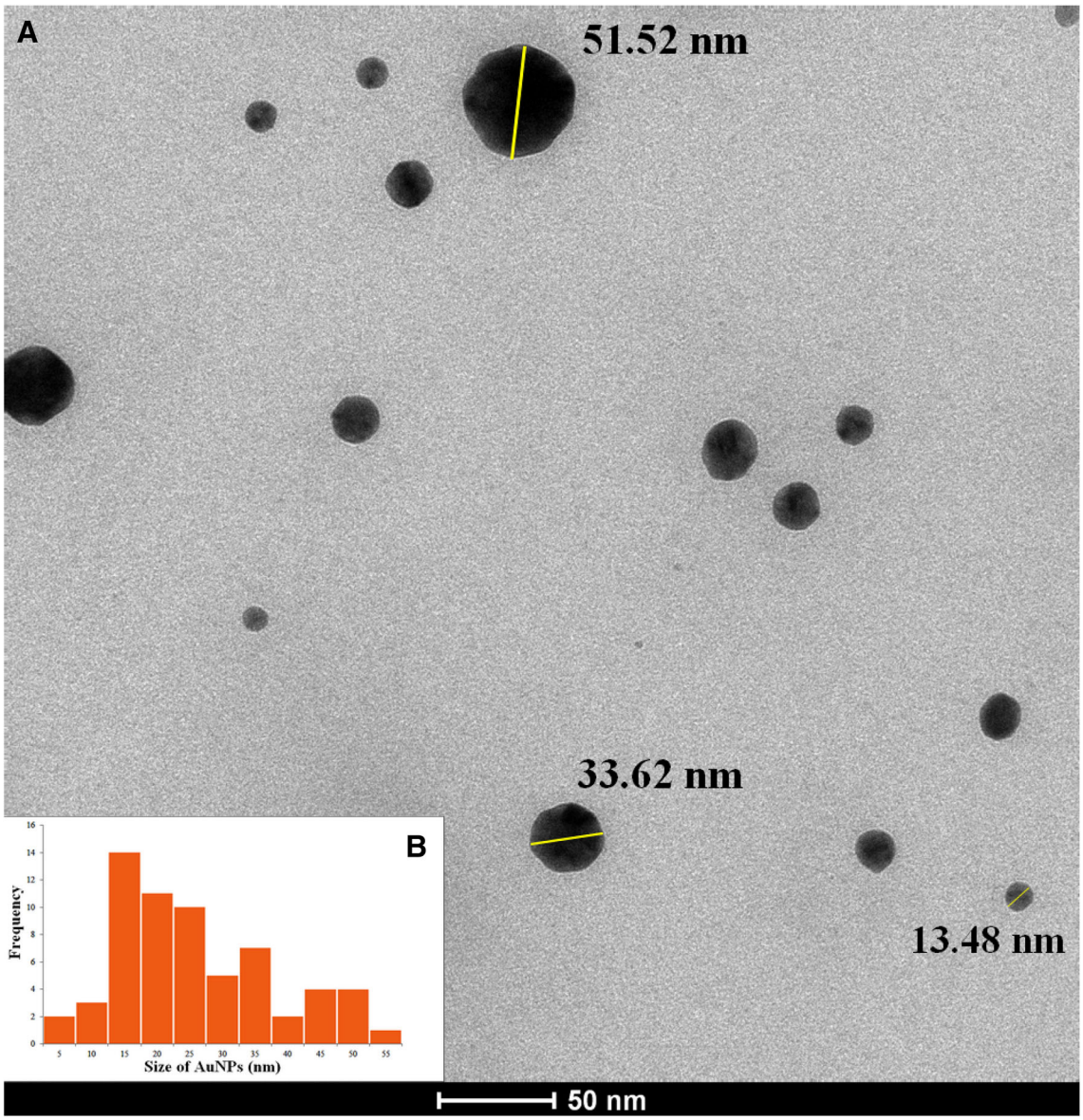

Fig. 4 TEM micrograph of gold nanoparticles at a scale bar of 50 nm (**a**) and particle size distribution histogram (**b**)

Conclusion

Marine flora and fauna are known to possess the capability of tolerating large fluctuations in many environmental parameters such as light, heat, pressure salinity and dissolved minerals or even gases. Hence, these organisms through millions of years of evolution have developed genomes that produce a wide variety of chemicals which have proved useful to man as medicines, cosmetics and agrochemicals. In the quest to identify different methods for the effective synthesis of metal nanoparticles, the marine ecosystem must be explored much further. Gold nanoparticles are exceptionally helpful because of their stability under different physiological conditions, imperviousness to oxidation and biocompatibility. This report has shown for the first time ever that, members of the genus *Mycobacterium* could be utilized for extracellular synthesis of gold nanoparticles. Gold nanoparticles synthesized by *Mycobacterium* sp. BRS2A-AR2 were spherical in shape and averagely sized at 11.8 nm. FT-IR spectrum confirmed the reduction and capping of AuNPs from which it can be inferred that the functional groups –COOH, –OH, and –NH could have caused the stabilization of the AuNPs. DLS analysis uncovered the size distribution of AuNPs in liquid. Zeta potential value (− 28.3 mV) has shown that the AuNPs are reliably stable. The most significant effects of AuNPs synthesized extracellularly on HUVEC and HeLA cell lines were determined statistically

at 3500 µg/ml concentrations. This article may consequently prompt the advancement of a straightforward, fast, clean and non-costly biomediated synthesis of AuNPs by marine *Actinobacteria*.

Acknowledgements KK wishes to thank Centre for African Wetlands (CAW), University of Ghana for providing seed funding to enable collection of samples. KK is grateful to Cambridge-Africa Partnership for Research Excellence (CAPREx)—funded by the Carnegie Corporation of New York, for a Postdoctoral Fellowship. KK also appreciates Cambridge-Africa ALBORADA Research Fund for support.

References

1. Narayanan KB, Sakthivel N (2010) Biological synthesis of metal nanoparticles by microbes. Adv Coll Interface Sci 156(1–2):1–13. https://doi.org/10.1016/j.cis.2010.02.001
2. Stark WJ, Stoessel PR, Wohlleben W, Hafner A (2015) Industrial applications of nanoparticles. Chem Soc Rev 44(16):5793–5805. https://doi.org/10.1039/c4cs00362d
3. Baetke SC, Lammers T, Kiessling F (2015) Applications of nanoparticles for diagnosis and therapy of cancer. Br J Radiol 88(1054):20150207. https://doi.org/10.1259/bjr.20150207
4. Diao F, Wang Y (2017) Transition metal oxide nanostructures: premeditated fabrication and applications in electronic and photonic devices. J Mater Sci 53(6):4334–4359. https://doi.org/10.1007/s10853-017-1862-3
5. Martins M, Mourato C, Sanches S, Noronha JP, Crespo MT, Pereira IA (2017) Biogenic platinum and palladium nanoparticles as new catalysts for the removal of pharmaceutical compounds. Water Res 108:160–168. https://doi.org/10.1016/j.watres.2016.10.071
6. Patel SKS, Lee J-K, Kalia VC (2017) Nanoparticles in biological hydrogen production: an overview. Indian J Microbiol. https://doi.org/10.1007/s12088-017-0678-9
7. Pugazhendhi S, Kirubha E, Palanisamy PK, Gopalakrishnan R (2015) Synthesis and characterization of silver nanoparticles from Alpinia calcarata by Green approach and its applications in bactericidal and nonlinear optics. Appl Surf Sci 357:1801–1808. https://doi.org/10.1016/j.apsusc.2015.09.237
8. De Sio L, Placido T, Comparelli R, Lucia Curri M, Striccoli M, Tabiryan N, Bunning TJ (2015) Next-generation thermo-plasmonic technologies and plasmonic nanoparticles in optoelectronics. Prog Quantum Electron 41:23–70. https://doi.org/10.1016/j.pquantelec.2015.03.001
9. Patel SK, Choi SH, Kang YC, Lee JK (2016) Large-scale aerosol-assisted synthesis of biofriendly Fe(2)O(3) yolk-shell particles: a promising support for enzyme immobilization. Nanoscale 8(12):6728–6738. https://doi.org/10.1039/c6nr00346j
10. Patel SK, Choi SH, Kang YC, Lee JK (2017) Eco-friendly composite of Fe3O4-reduced graphene oxide particles for efficient enzyme immobilization. ACS Appl Mater Interfaces 9(3):2213–2222. https://doi.org/10.1021/acsami.6b05165
11. Otari SV, Kumar M, Anwar MZ, Thorat ND, Patel SKS, Lee D, Lee JH, Lee JK, Kang YC, Zhang L (2017) Rapid synthesis and decoration of reduced graphene oxide with gold nanoparticles by thermostable peptides for memory device and photothermal applications. Sci Rep 7(1):10980. https://doi.org/10.1038/s41598-017-10777-1
12. Otari SV, Patel SKS, Jeong J-H, Lee JH, Lee J-K (2016) A green chemistry approach for synthesizing thermostable antimicrobial peptide-coated gold nanoparticles immobilized in an alginate biohydrogel. Rsc Adv 6(90):86808–86816. https://doi.org/10.1039/c6ra14688k
13. Khan ME, Khan MM, Cho MH (2015) Green synthesis, photocatalytic and photoelectrochemical performance of an Au–Graphene nanocomposite. Rsc Adv 5(34):26897–26904. https://doi.org/10.1039/c5ra01864a
14. Hulkoti NI, Taranath TC (2014) Biosynthesis of nanoparticles using microbes—a review. Colloids Surf B 121:474–483. https://doi.org/10.1016/j.colsurfb.2014.05.027
15. Golinska P, Wypij M, Ingle AP, Gupta I, Dahm H, Rai M (2014) Biogenic synthesis of metal nanoparticles from actinomycetes: biomedical applications and cytotoxicity. Appl Microbiol Biotechnol 98(19):8083–8097. https://doi.org/10.1007/s00253-014-5953-7
16. Thakkar KN, Mhatre SS, Parikh RY (2010) Biological synthesis of metallic nanoparticles. Nanomed-Uk 6(2):257–262. https://doi.org/10.1016/j.nano.2009.07.002
17. Barka EA, Vatsa P, Sanchez L, Gaveau-Vaillant N, Jacquard C, Klenk HP, Clement C, Ouhdouch Y, van Wezel GP (2016) Taxonomy, physiology, and natural products of actinobacteria. Microbiol Mol Biol Rev MMBR 80(1):1–43. https://doi.org/10.1128/MMBR.00019-15
18. Goodfellow M, Williams ST (1983) Ecology of actinomycetes. Annu Rev Microbiol 37:189–216. https://doi.org/10.1146/annurev.mi.37.100183.001201
19. Ramesh S, Jayaprakashvel M, Mathivanan N (2006) Microbial status in seawater and coastal sediments during pre- and post-tsunami periods in the Bay of Bengal, India. Mar Ecol 27(3):198–203. https://doi.org/10.1111/j.1439-0485.2006.00110.x
20. Ramesh S, Mathivanan N (2009) Screening of marine actinomycetes isolated from the Bay of Bengal, India for antimicrobial activity and industrial enzymes. World J Microbiol Biotechnol 25(12):2103–2111. https://doi.org/10.1007/s11274-009-0113-4
21. Zhang H, Zhang W, Jin Y, Jin M, Yu X (2008) A comparative study on the phylogenetic diversity of culturable actinobacteria isolated from five marine sponge species. Antonie Van Leeuwenhoek 93(3):241–248. https://doi.org/10.1007/s10482-007-9196-9
22. Das M, Royer TV, Leff LG (2007) Diversity of fungi, bacteria, and actinomycetes on leaves decomposing in a stream. Appl Environ Microbiol 73(3):756–767. https://doi.org/10.1128/AEM.01170-06
23. Karthik L, Kumar G, Keswani T, Bhattacharyya A, Reddy BP, Rao KVB (2013) Marine actinobacterial mediated gold nanoparticles synthesis and their antimalarial activity. Nanomed-Nanotechnol 9(7):951–960. https://doi.org/10.1016/j.nano.2013.02.002
24. Manivasagan P, Venkatesan J, Kang KH, Sivakumar K, Park SJ, Kim SK (2015) Production of alpha-amylase for the biosynthesis of gold nanoparticles using *Streptomyces* sp. MBRC-82. Int J Biol Macromol 72:71–78. https://doi.org/10.1016/j.ijbiomac.2014.07.045
25. Manivasagan P, Venkatesan J, Senthilkumar K, Sivakumar K, Kim SK (2013) Biosynthesis, antimicrobial and cytotoxic effect of silver nanoparticles using a novel nocardiopsis sp MBRC-1. Biomed Res Int. https://doi.org/10.1155/2013/287638
26. Singh R, Nawale LU, Arkile M, Shedbalkar UU, Wadhwani SA, Sarkar D, Chopade BA (2015) Chemical and biological metal nanoparticles as antimycobacterial agents: a comparative study. Int J Antimicrob Agents 46(2):183–188. https://doi.org/10.1016/j.ijantimicag.2015.03.014
27. Mansour A, Tammam S, Althani A, Azzazy HME (2017) A single tube system for the detection of Mycobacterium tuberculosis DNA using gold nanoparticles based FRET assay.

J Microbiol Methods 139:165–167. https://doi.org/10.1016/j.mimet.2017.06.001
28. Malhotra A, Dolma K, Kaur N, Rathore YS, Ashish Mayilraj S, Choudhury AR (2013) Biosynthesis of gold and silver nanoparticles using a novel marine strain of Stenotrophomonas. Bioresour Technol 142:727–731. https://doi.org/10.1016/j.biortech.2013.05.109
29. Lane DJ (1991) 16S/23S rRNA sequencing. Nucleic acid techniques in bacterial systematics. Wiley, Chichester, pp 115–175
30. Kim OS, Cho YJ, Lee K, Yoon SH, Kim M, Na H, Park SC, Jeon YS, Lee JH, Yi H, Won S, Chun J (2012) Introducing EzTaxon-e: a prokaryotic 16S rRNA gene sequence database with phylotypes that represent uncultured species. Int J Syst Evol Microbiol 62:716–721. https://doi.org/10.1099/ijs.0.038075-0
31. Tamura K, Stecher G, Peterson D, Filipski A, Kumar S (2013) MEGA6: molecular evolutionary genetics analysis version 6.0. Mol Biol Evol 30(12):2725–2729. https://doi.org/10.1093/molbev/mst197
32. Saitou N, Nei M (1987) The neighbor-joining method: a new method for reconstructing phylogenetic trees. Mol Biol Evol 4(4):406–425
33. Kluge AG, Farris JS (1969) Quantitative phyletics and the evolution of anurans. Syst Zool 18:1–32
34. Felsenstein J (1981) Evolutionary trees from DNA sequences: a maximum likelihood approach. J Mol Evol 17(6):368–376
35. Felsenstein J (1985) Phylogenies and the comparative method. Am Nat 125(1):1–15
36. Singh AK, Talat M, Singh DP, Srivastava ON (2010) Biosynthesis of gold and silver nanoparticles by natural precursor clove and their functionalization with amine group. J Nanopart Res 12(5):1667–1675. https://doi.org/10.1007/s11051-009-9835-3
37. George WO, McIntyre PS, Mowthorpe DJ (1987) ACOL (Project) Infrared spectroscopy. Analytical chemistry by open learning. Published on behalf of ACOL, London, by Wiley, Chichester West Sussex; New York